# Families of Fixed-Point Cellular Rotations

Lowell Abrams

*Department of Mathematics*
*The George Washington University*
*Washington, DC 20052*

**Abstract**

A *cellular rotation* is a pseudofree cellular automorphism, with no non-fixed pseudofixed points, of a graph embedded in an orientable surface. A *family* of cellular rotations is a collection of cellular rotations having one embedding of each genus above some fixed minimum genus, all sharing the same quotient embedding and, in an appropriate sense, the same voltage-assignment data. We provide a complete catalog of all families of cellular rotations having at least one fixed point, and provide preliminary results regarding families of cellular rotations having no fixed points.

*Keywords:* graph embedding, cellular automorphism, voltage assignment

## 1. Introduction

An embedding of a graph $G$ in a surface $S$ is *cellular* if the complement of $G$ in $S$ is a disjoint union of topological disks; all embeddings in this paper will be cellular. A *cellular automorphism* of a graph $G$ in $S$ is an automorphism of a graph $G$ embedded in $S$ which takes facial boundary walks to facial boundary walks. This paper uses techniques of the present author and Slilaty [1] to study families of cellular automorphisms called here "fixed-point cellular rotations."

While the work here is in a sense founded on [1], it differs in important respects. In [1], we provide complete catalogs of all irreducible cellular automorphisms of surfaces of Euler characteristic at least -1 ("irreducibility" is in terms of a type of graph minor which preserves the cellularity of the embedding and respects the action of the automorphism). Note that they fix a surface $S$ and discuss all possible automorphisms for that fixed $S$. Here, however, it is the quotient and lifting data (*i.e.*, voltage assignment) that are fixed, and the objects of study are families of all possible automorphisms for that fixed information. In [2], the present author and Slilaty find all minimal $\mathbb{Z}_n$-symmetric graphs that are not $\mathbb{Z}_n$-spherical; that work involves fixing a quotient, but there all lifts are in the same surface, whereas here we restrict attention to families

*Email address:* `labrams@gwu.edu` (Lowell Abrams)

that have one representative for each genus above a certain minimum genus (which depends on the family).

We now sketch the definition of family used in this paper; for more details, see Definition 3.1.1. In each family, all cellular automorphisms have the same quotient embedding: graph $\check{G}$ in surface $\check{S}$. This quotient embedding is equipped with a function $\alpha\colon E(\check{G}) \to \mathbb{Z}[w]/(aw+b)$ where $w$ is a variable and there is a fixed choice of $aw+b \in \mathbb{Z}[w]$. For each genus $g$ above some fixed minimum genus, the function $\alpha_g$ obtained from $\alpha$ by evaluating $w$ at $g$ yields a voltage assignment on $\check{G}$ in $\check{S}$, and the derived embedding is a member of the family.

Thus, one may loosely describe this paper as a study of families of cellular automorphisms in each of which family all members "are the same cellular automorphism for a different surface." Another way to say this is that in each family there is a strong "family resemblance" among its members. In addition to this, we restrict ourselves to "cellular rotations," which require that the only points of the surface which are not of full orbit under the action of the automorphism are fixed points.

Our main result is Theorem 3.3.2, which we summarize here:

**Main Theorem.** *There are only three main categories of families with at least one fixed point, as constructed explicitly in Section 3.2. Specifically, there are:*

- *9 families of order $g$ automorphisms of the genus $g$ surface having 2 fixed points and quotient surface the torus;*
- *2 families of order $2g+1$ automorphisms of the genus $g$ surface having 3 fixed points and quotient surface the sphere;*
- *3 families of order $g+1$ automorphisms of the genus $g$ surface having 4 fixed points and quotient surface the sphere.*

Our results below show, taking Proposition 3.3.1 and Theorem 4.1.1 together, that there is only one category of families with no fixed points; these consist of order $g-1$ automorphisms of the genus $g$ surface with quotient surface the torus. We do only an initial analysis of these families here.

The reader may wonder about automorphisms of order $2g$ or $2g-2$ of the genus $g$ surface which involve a rotation-reflection (glide reflection). Such automorphisms, however, cannot form a family according to our definition. For rotation-reflections, the corresponding quotient surface will depend on the parity of the genus, whereas our definition fixes the quotient surface and provides for an automorphism for each surface of sufficiently large genus (with the order of the automorphism depending linearly on the genus).

Section 2 provides the necessary background material in topological graph theory. Section 3 begins with a formal definition of "rotation family," provides a complete catalog of all rotation families having at least one fixed point, then proves completeness of the catalog. Section 4 provides a preliminary analysis of rotation families having no fixed points, and suggests an alternative approach towards studying such cellular automorphisms.

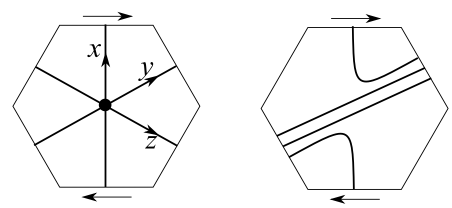


Figure 1: On the left is an embedding of $B_3$ in Dyck's (three crosscaps) surface, and on the right is a simple closed curve representing the Möbius walk $xy^{-3}$. Our convention when depicting topological surfaces is to identify opposite sides of a polygon, and to do this in an orientation-preserving manner unless there are arrows indicating otherwise.

## 2. Background material

### *2.1. Cellular embeddings and cellular automorphisms*

Given a graph $G$ with vertex set $V(G)$ and edge set $E(G)$, we view each edge $e$ as directed, *i.e.*, as having a source-vertex and a target-vertex, and write "$e^{-1}$" for the same edge but with source and target reversed. When using directed edges we will write $\overrightarrow{E}$ for emphasis.

A *cellular embedding* of a graph $G$ in a topological surface $S$, which we denote $G \to S$, is an embedding of the graph as a 1-dimensional topological space such that the complement of $G$ in $S$ is a disjoint union $F(G)$ of contractible open cells. Given a cellular embedding of $G$ in $S$, we will make frequent use of walks in $G$ to refer to curves in $S$. When a closed walk $W$ in $G$ can be topologically represented by a simple closed curve in $S$, we will call $W$ an *annular walk* if it has a neighborhood homeomorphic to an annulus, and a *Möbius walk* if it has a neighborhood homeomorphic to a Möbius band. If surface $S$ is nonorientable, then $G$ in $S$ necessarily has at least one Möbius walk. Given a sequence of edges $e_1, e_2, \ldots, e_r$ (by assumption, directed) such that for each $i$ the target of $e_i$ is the source of $e_{i+1}$ (subscripts taken modulo $r$), we will denote the corresponding walk in $G$ by $e_1 e_2 \cdots e_r$.

See Figure 1 for an example of a Möbius walk and the corresponding simple closed curve.

A *cellular automorphism* of a graph $G$ in a surface $S$ is a function $\varphi$ on $V(G) \amalg \overrightarrow{E} \amalg F(G)$ which sends vertices to vertices, edges to edges, and faces to faces in an adjacency and incidence-preserving manner. In particular, any cellular automorphism $\varphi$ restricts to an automorphism of $G$. We write $|\varphi|$ for the order of $\varphi$, and $G/\langle\varphi\rangle$ and $S/\langle\varphi\rangle$ for the quotients of $G$ and $S$, respectively, by the action of $\varphi$. A *pseudofixed point* of $\varphi$ is a point of $S$ that is fixed by $\varphi^k$ for some $k \geq 1$.

**Definition 2.1.1.** A *cellular rotation* of a graph $G$ in a surface $S$ is a cellular automorphism which acts freely on the vertices and edges of the embedding and whose pseudofixed points are all isolated fixed points in the centers of faces. A *fixed-point cellular rotation* is a cellular rotation which is not free.

Note that this definition does not require preserving orientation, so includes rotation-reflections (glide reflections). The goal of this paper is to study certain families of cellular rotations, as defined in Section 3.1 and listed in Section 3.2.

We now review some definitions from [1], where they are dealt with in detail. Our definitions here are actually somewhat simplified by our assumptions regarding fixed points. Let $\varphi$ be an automorphism of $G$, not necessarily free, and for $C \subset E(G)$ write $\mathsf{orbit}_\varphi(C)$ for the orbit of $C$ under the action of $\varphi$. For a subset $X \subset E(G)$ we write $G\backslash X$ for the result of deleting $X$ from $G$, and $G/X$ for the result of contracting $X$. In this paper we work with multigraphs, so any loops and parallel edges introduced when contracting edges are retained. Given $C, D \subset E(G)$ with $\mathsf{orbit}_\varphi(C) \cap \mathsf{orbit}_\varphi(D) = \emptyset$ we call the minor $H = G/\mathsf{orbit}_\varphi(C)\backslash\mathsf{orbit}_\varphi(D)$ an *orbit minor* of $G$ with respect to $\varphi$; observe that an orbit minor of $G$ is a cover of a minor of the quotient of $G$ under the action of $\varphi$. The automorphism $\varphi$ naturally induces an automorphism $\varphi|_H$ of $H$.

Now let $\varphi$ be a cellular automorphism of $G$ in $S$, again not necessarily free on $G$, and let $C, D \subset E(G)$ be such that

- $\mathsf{orbit}_\varphi(C) \cap \mathsf{orbit}_\varphi(D) = \emptyset$,
- the subgraph of $\mathsf{orbit}_\varphi(C)$ in $G$ is acyclic,
- $G\backslash\mathsf{orbit}_\varphi(D)$ is connected and cellularly embedded in $S$, and
- each fixed point of $\varphi$ is the center of a distinct face.

When these hold we call $G/\mathsf{orbit}_\varphi(C)\backslash\mathsf{orbit}_\varphi(D)$ a *surface orbit minor* with respect to $\varphi$. As with orbit minors, we can describe a surface orbit minor in terms of a minor of the quotient embedding, but being careful to only work with minors of the quotient that preserve the quotient surface. The automorphism $\varphi$ naturally induces an automorphism $\varphi|_H$ of $H$ in $S$.

We call a cellular embedding of a graph $G$ in a surface $S$ *irreducible* if it has no nontrivial surface orbit minors (when no automorphism $\varphi$ of $G$ in $S$ is specified, we take $\varphi$ to be the identity). For instance, if $B_k$ is the *$k$-loop bouquet*, *i.e.,* the graph with a single vertex and $k$ loops, with the trivial automorphism, then a cellular embedding of $B_{2g}$ in an orientable genus $g$ surface is necessarily irreducible. On the other hand, suppose $\varphi$ is an automorphism of $B_{2g+1}$ in the genus $g$ surface. If $\varphi$ is the identity map, then the embedding is not irreducible, since we can delete a loop, but when $\varphi$ is pseudofree with two fixed points and no other pseudofixed points, the embedding is in fact irreducible since each of the two faces has a fixed point in its center.

### *2.2. Voltage assignments and derived embeddings*

Let $A$ be a finite abelian group of order $|A|$; we write all group operations as additions. Furthermore, for $a \in A$, let $|a|$ denote the order of $a$ in $A$. An $A$-voltage assignment to a graph $G$ is a function $\sigma\colon \vec{E}(G) \to A$ such that $\sigma(e^{-1}) = -\sigma(e)$ for all $e \in \vec{E}(G)$. The pair $(G, \sigma)$ is a *voltage graph*. Given voltage graph

$(G,\sigma)$, the *derived graph* $G^\sigma$ has vertex set $V(G)\times A$ and edge set $\vec{E}(G^\sigma) = \vec{E}(G)\times A$, where if $e\in \overrightarrow{E}(G)$ is an edge from $u$ to $v$, then $(e,a)\in \overrightarrow{E}(G^\sigma)$ is an edge from $(u,a)$ to $(v,a+\sigma(e))$.

If voltage graph $(G,\sigma)$ is cellularly embedded in surface $S$, then tracing the entire boundary of a face $f$ of $G$ in $S$ yields a closed walk in $G$ called a *boundary walk* of $f$. We refer to a face with a particular choice of boundary walk as an *oriented face*, and for each oriented face $f$ we let $\partial f$ denote the chosen walk. Also, for each walk $W = e_1e_2\cdots e_k$ we let $\sigma(W)$ denote the *total voltage of* $W$, *i.e.*, the sum $\sum_i \sigma(e_i)$. For an oriented face $f$, we call $\sigma(\partial f)$ the *total voltage on* $f$; since $A$ is abelian this is independent, up to sign, of choice of boundary walk.

For each oriented face $f$ of $G$ in $S$, the edges $(e,a)\in \overrightarrow{E}(G^\sigma)$ such that $e\in\partial f$ comprise a disjoint collection of $|A|/|\sigma(\partial f)|$ closed walks in $G^\sigma$. Attaching a 2-cell to each of these closed walks, for each oriented face $f$, yields a cellular embedding of $G^\sigma$ in a surface we denote by $S^\sigma$, called the *derived surface.*

The following well known results will be useful below.

**Proposition 2.2.1** ([1, Prop. 2.1] and [6])**.** *If $G$ is cellularly embedded in surface $S$ and $\sigma,\tau$ are $A$-voltage assignments on $G$ such that for any cycle $C$ in $G$ the total $\sigma$-voltage on $C$ equals the total $\tau$-voltage on $C$, then there is an isomorphism of derived embeddings $G^\sigma \to S^\sigma$ and $G^\tau \to S^\tau$.*

**Proposition 2.2.2** ([3])**.** *Given cellular embedding $G\to S$ and $A$-voltage assignment $\sigma$ on $G$, the derived surface $S^\sigma$ will be nonorientable if and only if there is some Möbius walk in $G$ whose total voltage has odd order in $A$.*

Proposition 2.2.3 is a special case of a well known result from Gvozdjak and Širáň [4].

**Proposition 2.2.3.** *Consider a cellular embedding $G\to S$ and suppose $\sigma$ and $\tau$ are $A$-voltage assignments on $G$.*

1. *If $\varphi$ is a cellular automorphism of $G$ in $S$ such that $\tau = \sigma\circ\varphi$, then there is a cellular isomorphism of $G^\sigma\to S^\sigma$ to $G^\tau\to S^\tau$.*
2. *If $\zeta$ is an automorphism of $A$ such that $\tau = \zeta\circ\sigma$, then there is a cellular isomorphism of $G^\sigma\to S^\sigma$ to $G^\tau\to S^\tau$.*

*Proof.* By [4], the cellular automorphism $\varphi$ in Item 1 lifts to a cellular automorphism of derived embeddings if and only if for every closed walk $W$ we have

$$\tau(W) = 0 \iff \sigma\circ\varphi(W) = 0.$$

Under the hypotheses of our proposition, this condition is trivially satisfied. In Item 2 we apply [4] with $\varphi = \mathrm{id}$, and again the condition is trivially satisfied. □

If $\sigma$ is a $\mathbb{Z}_n$-voltage assignment on graph $G$ in surface $S$, there is a naturally induced cellular automorphism $\varphi_\sigma$ on the derived embedding $G^\sigma\to S^\sigma$, which we call the *natural automorphism*, given by mapping $(v,k)\mapsto(v,k+1)$ and $(e,k)\mapsto(e,k+1)$ for each vertex $v$ and edge $e$ of $G$, and each voltage $k$. Notice that the action of $\varphi_\sigma$ is free on the graph $G^\sigma$, and any pseudofixed points are located in the centers of faces. In particular, if $f$ is an oriented face such that $\sigma(\partial f) \neq 0$, then $\varphi_\sigma$ has a pseudofixed point in the center of $f$ which is fixed by $(\varphi_\sigma)^{n/|\sigma(\partial f)|}$. Taking $\pi\colon S^\sigma \to S$ to denote the natural covering map, we see that the branch points of $\pi$ are the centers of those oriented faces $f$ of $G$ in $S$ having $\sigma(\partial f) \neq 0$, and the pseudofixed points of $\varphi_\sigma$ are the prebranch points. Moreover, when all pseudofixed points are isolated fixed points it must be that all oriented faces $f$ have $|\sigma(\partial f)| \in \{1, n\}$. This, together with our requirements regarding pseudofixed points and the results of [1, §3.2], gives the following useful result.

**Proposition 2.2.4.** *If $\varphi_\sigma$ is an irreducible order $n$ cellular automorphism of $G^\sigma$ in $S^\sigma$ with $k$ fixed points, $k \neq 0$, and $S$ has genus $g$, then $G = B_{2g+k-1}$ and $|\sigma(\partial f)| = n$ for every oriented face $f$ of $G$ in $S$.*

*Proof.* Recall first the observation from Section 2.1 that surface orbit minors correspond to minors of the quotient surface. Accordingly, if any orbit of edges of $G^\sigma$ can be contracted, then below in the quotient $G$ one can contract a spanning tree. Thus, the quotient graph for an irreducible cellular automorphism has only a single vertex. If any orbit of edges in the embedding above can be deleted, below in the quotient one can delete edges between faces that do not both contain a branch point. Thus, the quotient graph for an irreducible cellular automorphism has a branch point (in this case, a fixed point) in each face. □

For a surface $S$, we let $\chi(S)$ denote the Euler characteristic of $S$. The following is a specialized formulation of the Riemann-Hurwitz Theorem [3, §6.3.1].

**Proposition 2.2.5.** *Let $G$ be cellularly embedded in surface $S$, let $\sigma$ be a $\mathbb{Z}_n$-voltage assignment on $G$, and let $f_1, \ldots, f_k$ be the distinct oriented faces of $G$ in $S$ with $\sigma(\partial f_i) \neq 0$. Then*

$$\chi(S^\sigma) = n\chi(S) - \sum_{i=1}^{k} \left( n - \frac{n}{|\sigma(\partial f_i)|} \right).$$

## 3. Rotation Families With Fixed Points

### *3.1. Rotation families*

We begin with an explanatory example. Let $\check{G} \to \check{S}$ denote the embedding of the two-loop bouquet in the sphere shown in Figure 3. We would like to use a voltage assignment approach to construct an infinite family of embeddings, one for each surface of genus $g \geq 1$, which all have $\check{G} \to \check{S}$ as quotient embedding. Of course, the voltage assignments cannot strictly be the same, since in each case the order of the voltage group will be different. But to achieve a notion of sameness across all the voltage assignments, we use $\mathbb{Z}[w]/(2w+1)$ as a universal stand-in for the groups $\mathbb{Z}_{2g+1}$. Thus, we define $\alpha\colon E(\check{G}) \to \mathbb{Z}[w]/(2w+1)$ by $\alpha(x) := 1$ and $\alpha(y) := w$. For each $g \geq 1$, evaluating at $w = g$ yields a specific voltage assignment $\alpha_g\colon E(\check{G}) \to \mathbb{Z}_{2g+1}$ given by $(\alpha_g(x), \alpha_g(y)) = (1, g)$, with corresponding derived embedding in the surface of genus $g$.

We now introduce the main definition of this paper. We assume $\mathbb{N}$ contains 0.

**Definition 3.1.1.** A *rotation family* is a four-tuple $(k, \check{G} \to \check{S}, aw + b, \alpha)$ with

- $k \in \mathbb{N}$ and $aw + b \in \mathbb{Z}[w]$;
- $\check{G} \to \check{S}$ is an irreducible cellular embedding of a graph $\check{G}$ in a surface $\check{S}$;
- $\alpha$ is a function $\alpha\colon E(\check{G}) \to \mathbb{Z}[w]/(aw + b)$;
- There is $g_0 \in \mathbb{N}$ such that for each $g$ in $\mathbb{N}_{\geq g_0}$ the map $\alpha_g(\cdot) := \alpha(\cdot)|_{w=g}$ gives a $\mathbb{Z}_{ag+b}$-voltage assignment satisfying:
  - For each $e \in E(\check{G})$ there is a linear function $m_e\colon \mathbb{N}_{\geq g_0} \to \mathbb{N}$ such that the order of $\alpha_g(e)$ in $\mathbb{Z}_{ag+b}$ is $m_e(g)$;
  - The derived surface $\check{S}^{\alpha_g}$ is orientable of genus $g$;
  - The corresponding natural cellular automorphism $\varphi_g = \varphi_{\alpha_g}$ of $\check{G}^{\alpha_g} \to \check{S}^{\alpha_g}$ is a cellular rotation with exactly $k$ fixed points.

When $(k, \check{G} \to \check{S}, aw + b, \alpha)$ is a rotation family we will refer to each derived embedding of $G^{\alpha_g}$ in the genus $g$ surface as an *order $ag + b$ symmetry with $k$ fixed points*, and will speak of these derived embeddings as the "members" of the rotation family. Note that, in all cases, the natural automorphism acting on the derived embedding is a $\mathbb{Z}_n$ action, for some $n$, arising from a $\mathbb{Z}_n$-voltage assignment.

It will be useful to also have a more explicit notation for a rotation family. Given a rotation family $(k, \check{G} \to \check{S}, aw + b, \alpha)$ where $\check{S}$ is of genus $\check{g}$, Proposition 2.2.4 tells us that since $\check{G} \to \check{S}$ is irreducible and there are $k$ fixed points (and no other pseudofixed points), it must be that $\check{G}$ is a bouquet of $2\check{g} + k - 1$ loops $e_1, e_2, \ldots, e_{\check{g}+k-1}$. Further note that, given $(\check{g}, k)$, the embedding $\check{G} \to \check{S}$ is determined by the set $F$ of facial boundary walks. Thus, we denote the rotation family in question by $\mathcal{R}\big[(\check{g}, k), F;\ \ \mathbb{Z}_{ag+b},\ \big(\alpha_g(e_1),\ \ \alpha_g(e_2), \ldots,\ \ \alpha_g(e_k)\big)\big]$.

Notice that, by definition, $|\varphi_g|$ is a linear function $ag + b$ of $g$; for fixed $k$ and $\check{G} \to \check{S}$ this is in fact necessary. Explicitly, if $\varphi$ is a cellular rotation of some graph in surface $S$ of genus $g$ that has exactly $k$ fixed points and such that the quotient surface $S/\langle\varphi\rangle$ has Euler characteristic $2 - 2\check{g}$, then by Proposition 2.2.5 we have

$$2 - 2g = |\varphi|(2 - 2\check{g}) - k(|\varphi| - 1). \tag{1}$$

Since $k$ and $\check{g}$ are fixed, we see that $|\varphi|$ depends linearly on $g$.

The condition that the order of $\alpha_g(e)$ is given by a linear function $m_e(g)$ increases the "family resemblance" among the members of the rotation family. Otherwise, for instance, $\alpha_g(e)$ might be a generator of $\mathbb{Z}_{ag+b}$ for only some values of $g$ and not for others. While the formal framework demands working with the voltage assignment and the embedding of the voltage graph, it is the

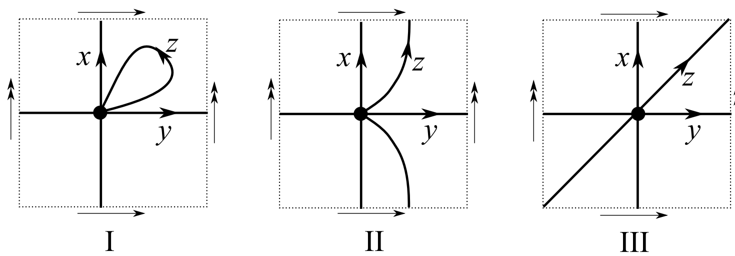


Figure 2: The embeddings of $B_3$ in $\mathbf{T}$ [5].

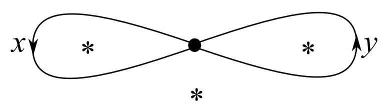


Figure 3: The embedding of $B_2$ in the sphere.

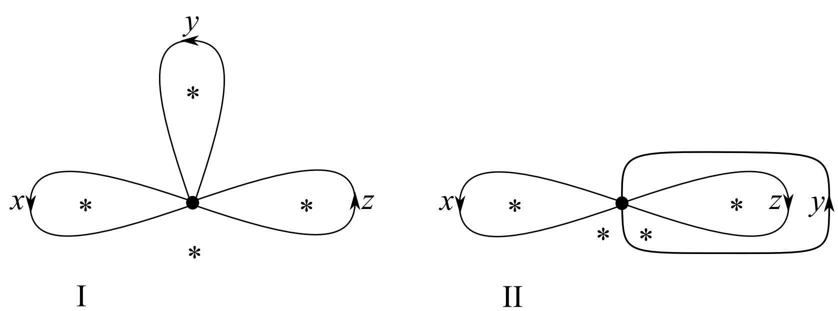


Figure 4: The embeddings of $B_3$ in the sphere.

members of the rotation family and their strong mutual similarity that are the true interest here.

*3.2. The Catalog*

We now list the rotation families with at least one fixed point. A series of figures at the end of this paper, as referenced below, depict an example from each family.

♦ $\mathcal{R}\big[(1,2),\ \{xy^{-1}x^{-1}z^{-1}y, z\};\, \mathbb{Z}_g,\ (1,1,1)\big]$
$\mathcal{R}\big[(1,2),\ \{xy^{-1}x^{-1}z^{-1}y, z\};\, \mathbb{Z}_g,\ (1,-1,1)\big]$
$\mathcal{R}\big[(1,2),\ \{xy^{-1}x^{-1}z^{-1}y, z\};\, \mathbb{Z}_g,\ (0,1,1)\big]$
$\mathcal{R}\big[(1,2),\ \{xy^{-1}x^{-1}z^{-1}y, z\};\, \mathbb{Z}_g,\ (0,0,1)\big]$

These families have $\check{G} \to \check{S}$ given by embedding I in Figure 2, and we may take $g_0 \geq 2$. Examples for $g = 3$ are shown in Figure 9, at the end of the paper.

♦ $\mathcal{R}\big[(1,2),\ \{xy^{-1}z^{-1}y, x^{-1}z\};\ \mathbb{Z}_g,\ (1,1,0))\big]$
$\mathcal{R}\big[(1,2),\ \{xy^{-1}z^{-1}y, x^{-1}z\};\ \mathbb{Z}_g,\ (1,-1,0)\big]$
$\mathcal{R}\big[(1,2),\ \{xy^{-1}z^{-1}y, x^{-1}z\};\ \mathbb{Z}_g,\ (1,0,0)\big]$

These families have $\check{G} \to \check{S}$ given by embedding II in Figure 2, and we may take $g_0 \geq 2$. Examples for $g = 3$ are shown in Figure 10.

♦ $\mathcal{R}\big[(1,2),\ \{xz^{-1}y, x^{-1}zy^{-1}\};\ \mathbb{Z}_g,\ (1,1,1)\big]$
$\mathcal{R}\big[(1,2),\ \{xz^{-1}y, x^{-1}zy^{-1}\};\ \mathbb{Z}_g,\ (0,0,1)\big]$

These families have $\check{G} \to \check{S}$ given by embedding III in Figure 2, and we may take $g_0 \geq 2$. Examples for $g = 3$ are shown in Figure 11.

♦ $\mathcal{R}\big[(0,3),\ \{x, y, x^{-1}y^{-1}\};\ \mathbb{Z}_{2g+1},\ (1,1)\big]$
$\mathcal{R}\big[(0,3),\ \{x, y, x^{-1}y^{-1}\};\ \mathbb{Z}_{2g+1},\ (1,g)\big]$

These families have $\check{G} \to \check{S}$ as given by Figure 3, and we may take $g_0 \geq 1$. Examples for $g = 2$ are shown as branched immersions in Figure 12.

♦ $\mathcal{R}\big[(0,4),\ \{x, y, z, x^{-1}y^{-1}z^{-1}\};\ \mathbb{Z}_{g+1},\ (1,1,-1)\big]$

This family have $\check{G} \to \check{S}$ as given by embedding I of Figure 4, and we may take $g_0 \geq 1$. An example for $g = 1$ is shown on the left of Figure 13 and an example for $g = 2$ is shown in Figure 14.

♦ $\mathcal{R}\big[(0,4),\ \{x, yz, z^{-1}, x^{-1}y^{-1}\};\ \mathbb{Z}_{g+1},\ (1,0,1)\big]$
$\mathcal{R}\big[(0,4),\ \{x, yz, z^{-1}, x^{-1}y^{-1}\};\ \mathbb{Z}_{g+1},\ (1,0,-1)\big]$

These families have $\check{G} \to \check{S}$ as given by embedding II of Figure 4, and we may take $g_0 \geq 1$. The case of $g = 1$ is the same for both families; this is depicted on the right of Figure 13. Examples for $g = 2$ are shown in Figure 14.

*3.3. Completeness of the Catalog*

We begin by analyzing Equation (1) from Section 3.1 a little more closely. If $(k, \breve{g}) = (2, 0)$ then (1) gives $g = 0$. If $(k, \breve{g}) = (0, 1)$ then (1) gives $|\varphi_g| = 2 - 2g$, but since $|\varphi_g| \geq 1$ we have $g \leq 1/2$. Thus, in either case we have a contradiction to the fact that we have a rotation family, since that requires allowing for infinitely many values of $g$. Given that $(k, \breve{g}) \neq (2, 0), (0, 1)$, we can solve for $|\varphi_g|$ in (1) to obtain

$$|\varphi_g| \ = \ \frac{2g - 2 + k}{2\breve{g} - 2 + k}. \tag{2}$$

As we use (2), observe that if $\check{S}$ is an orientable surface of genus $g$, then $\breve{g}$ will equal the genus of $\check{S}$, and otherwise $\breve{g}$ will denote one half the quantity of crosscaps in an "all-crosscaps" representation of $\check{S}$.

**Proposition 3.3.1.** *If* $(k, \check{G} \to \check{S}, aw+b, \alpha)$ *is a rotation family and* $\check{G}$ *has Euler characteristic* $2-2\check{g}$*, then the triple* $(k, \check{g}, ag+b)$ *is one of*

$$(0, \tfrac{3}{2}, 2g-2), (0, 2, g-1), (2, \tfrac{1}{2}, 2g), (2, 1, g), (3, 0, 2g+1), \text{ and } (4, 0, g+1).$$

*Proof.* Note first that $ag+b = |\varphi_g|$, so by Equation (2) it suffices to determine the possible pairs $(k, \check{g})$. Also, recall that if $\check{S}$ is orientable then $\check{g}$ is a nonnegative integer, but if $\check{S}$ is nonorientable then $\check{g}$ is of the form $n/2$ for some nonnegative integer $n$; it suffices initially to consider the latter. Note that the right hand side of (2) must give a positive integer for every value of $g \geq g_0$; this is a strong requirement, and we will use it repeatedly. We analyze cases according to values of $k$:

**Case** $k = 0$**:** Equation (2) gives

$$|\varphi_g| = \frac{g-1}{\check{g}-1} = \frac{g-1}{n/2-1} = \frac{2(g-1)}{n-2}.$$

Since $\varphi_g$ is an integer, either $n-2=1$ or, since we cannot have $(n-2)|(g-1)$ for all $g$, it must be that $(n-2)=2$. In the first case we get $\check{g} = \frac{3}{2}$ and in the second case $\check{g} = 2$.

**Case** $k = 1$**:** By definition we only consider automorphisms $\varphi_g$ of orientable surfaces. Thus, by [3, Theorem 4.3.7], this case is not possible.

**Case** $k = 2$**:** Equation (2) gives $|\varphi_g| = g/\check{g} = 2g/n$. Since $g$ may be relatively prime to $n$, we have either $n=1$ or $n=2$, *i.e.*, either $\check{g} = 1/2$ or $\check{g} = 1$.

**Case** $k \geq 3$**:** Writing $k = 2+d$ where $d \geq 1$, we have $|\varphi_g| = (2g+d)/(2\check{g}+d)$. Consider values of $g$ of the form $g = r(2\check{g}+d)$ where $r$ is an integer large enough that $g > g_0$. For such values of $g$ we have

$$|\varphi_g| = \frac{2r(2\check{g}+d)+d}{2\check{g}+d} = 2r + \frac{d}{2\check{g}+d}.$$

Since this is an integer, we have $(2\check{g}+d)|d$, which can only hold if $\check{g} = 0$. Equation (2) then becomes

$$|\varphi_g| = \frac{2g+d}{d} = \frac{2g}{d} + 1.$$

If $d=2$ then we get $k=4$ and $\check{g}=0$. Otherwise, let $d' = d$ if $2 \nmid d$, in which case $|\varphi_g| = (2g/d')+1$, and let $d' = d/2$ if $2|d$, in which case $|\varphi_g| = (g/d')+1$. We must have $d'|g$ for all $g$, but this is possible only if $d'=1$. Since $d \neq 2$ we must have $d = d' = 1$, and we get $k=3$ and $\check{g}=0$. □

**Theorem 3.3.2.** *The catalog given in Section 3.2 is a complete catalog of rotation families having at least one (hence at least two) fixed points.*

We begin with a few useful preliminary results.

**Lemma 3.3.3.** *Suppose fixed $g_0 \in \mathbb{N}$, $a \in \{1,2\}$, and $r, s, b \in \mathbb{Z}$ are such that $(r,s) \neq (0,0)$ and, for all $g \geq g_0$, the order of $rg+s$ in $\mathbb{Z}_{ag+b}$ is a linear function of $g$. Given $x \in \mathbb{Z}$ we write $[x]$ for the class of $x$ module $ag+b$.*

1. *If $ag+b = 2g-2\beta$, where $\beta \in \{0,1\}$ and the order of $rg+s$ is even for all $g \geq g_0$, then $[rg+s] \in \{[g-\beta], [\pm 1]\}$.*
2. *If $ag+b \in \{g, g-1, g+1\}$, then $[rg+s] \in \{[\pm 1]\}$.*
3. *If $ag+b = 2g+1$, then $[rg+s] \in \{[\pm g]\} \cup \{[\pm 2^t] | t \geq 0\}$.*

*Proof.* We first remind the reader that the order of $rg+s$ in $\mathbb{Z}_{ag+b}$ is

$$|rg+s| \;=\; \frac{ag+b}{\gcd(rg+s, ag+b)}.$$

We assume the order of $rg+s$ in $\mathbb{Z}_{ag+b}$ is a linear function $f(g)$; we will use the relation

$$ag+b = \gcd(rg+s, ag+b) f(g)$$

repeatedly. Also, note that since $a \in \{1,2\}$, any element $rg+s$ has a representative $r'g+s'$ modulo $ag+b$ with $r' < 2$. Thus we can take $r \in \{0,1\}$ without loss of generality.

*Proof of* (1): We write $ag+b = 2g-2\beta$, where $\beta \in \{0,1\}$. Assume that for all $g \geq g_0$, $f(g)$ is even. For $r=0$ we have

$$2g-2\beta = \gcd(s, 2g-2\beta) f(g).$$

Now if $s$ is even then $\gcd(s, 2g-2\beta) = 2$ for multiple values of $g$, which will force $f(g) = g-\beta$ in those cases, and hence in all cases. This is a contradiction, because $f(g)$ is supposed to be even for all $g \geq g_0$. It then follows that $s$ is odd so $\gcd(s, 2g-2\beta) = 1$ for multiple values of $g$, which forces $f(g) = 2g-2\beta$ for all $g$. But then $\gcd(s, 2g-2\beta) = 1$ for all $g$, so $[rg+s] = [s] = [\pm 1]$.

For $r=1$ we have

$$2g-2\beta = \gcd(g+s, 2g-2\beta) f(g). \tag{3}$$

We clearly have $rg+s = g+s = g-\beta$ as a possible solution. Suppose, then, that $s \neq -\beta$. Choose $g > g_0$ such that $g+s$ is odd and $\gcd(s+\beta, g-\beta) = 1$. We then have

$$\begin{aligned} 2g-2\beta = \gcd(g+s, 2g-2\beta) f(g) &= \gcd(g+s, g-\beta) f(g) \\ &= \gcd((g+s)-(g-\beta), g-\beta) f(g) \\ &= \gcd(s+\beta, g-\beta) f(g) \\ &= f(g). \end{aligned}$$

Since there are multiple such values of $g$, we have $f(g) = 2g-2\beta$ for all $g$. But then Equation (3) gives $\gcd(g+s, 2g-2\beta) = 1$ for all $g$, which is a contradiction since $g+s$ is even for some values of $g$. Thus, when $r=1$, we have $[rg+s] = [g-\beta]$.

*Proof of* (2): Suppose $ag+b \in \{g, g-1, g+1\}$; in these cases we may take $r=0$, so $s \neq 0$ and we have $ag+b = \gcd(s, ag+b)f(g)$. Since, in all cases, $ag+b$ takes on all values greater than $ag_0+b$, there are multiple values of $g$ for which $\gcd(s, ag+b) = 1$. We can therefore conclude as above that $\gcd(s, ag+b) = 1$ for all $g$, and hence that $[rg+s] = [s] = [\pm 1]$.

*Proof of* (3): Now suppose that $ag+b = 2g+1$. For $r=0$ we have $s \neq 0$ and $2g+1 = \gcd(s, 2g+1)f(g)$. Since $2g+1$ takes on all odd values greater than $2g_0+1$, there are multiple values of $g$ for which $\gcd(s, 2g+1) = 1$. As above, we conclude that $\gcd(s, 2g+1) = 1$ for all $g$, and thus $[rg+s] = [s] \in \{[\pm 2^t] | t \geq 0\}$.

For $r=1$ we have

$$\begin{aligned} 2g+1 \; = \; \gcd(g+s, 2g+1)f(g) \;&=\; \gcd(g+s, 2g+1-2(g+s))f(g) \\ &=\; \gcd(g+s, 1-2s)f(g). \end{aligned}$$

As above, by considering special values of $g$ we can conclude that $\gcd(g+s, 1-2s) = \gcd(g+s, 2s-1) = 1$ for all $g$. For $g$ of the form $t|2s-1|-s > g_0$ we have

$$1 = \gcd(g+s, 2s-1) = \gcd(t|2s-1|, 2s-1) = |2s-1|,$$

and thus $s \in \{0,1\}$; of course, these values of $s$ work for all $g$. Thus $[rg+s] \in \{[g], [g+1]\} = \{[\pm g]\}$ when $r=1$, and for $ag+b = 2g+1$ we have $[rg+s] \in \{[\pm g]\} \cup \{[\pm 2^t] | t \geq 0\}$. $\square$

Note that all of the automorphisms being catalogued in this paper are constructed as the natural automorphism corresponding to a derived embedding, and we consider only cellular automorphisms of orientable surfaces. It therefore follows from Proposition 2.2.2 that every Möbius walk in the base graph must have total voltage of even order in $\mathbb{Z}_n$, and thus $n$ must be even. We arrive at the following observation.

**Observation 3.3.4.** *When constructing a rotation family* $\mathcal{R}\big[(\breve{g}, k), F; \mathbb{Z}_{ag+b}, \ldots\big]$ *for which* $ag+b$ *is odd, we need not consider any nonorientable quotient surfaces.*

We now prove our main theorem. Note that we make frequent use of Jackson and Visentin's atlas of graph embeddings [5]. Also, a comment about methodology is in order. At various points in the proof we use the presence of particular Möbius walks, as well as other calculations, to eliminate certain cases from consideration. Because we construct examples in all cases not eliminated by our analysis, we can be assured that no further constraints are present.

*Proof of Theorem 3.3.2.* We break the proof into cases according to the possible triples $(k, \breve{g}, ag+b)$ as identified in Proposition 3.3.1 which have $k > 0$. In all cases we require irreducible base embeddings and that all pseudofixed points are fixed, so by Proposition 2.2.4 we consider only embeddings of $B_r$, for some $r$, and we require $\sigma(\partial f)$ have maximum possible order for all oriented faces $f$.

Finally, note that all computations making use of Lemma 3.3.3 are to be taken modulo the relevant value of $ag+b$.

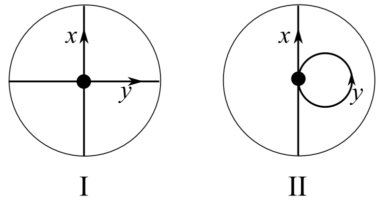


Figure 5: The embeddings of $B_2$ in the projective plane.

**Case** $(k, \breve{g}, ag+b) = (2, \frac{1}{2}, 2g)$**:**

Since $\breve{g} = \frac{1}{2}$, the surface $\breve{S}$ is the projective plane $\mathbf{P}$. Because $k = 2$ we require a two-faced irreducible embedding. We consider in turn each of the two possible embeddings of $B_2$ in $\mathbf{P}$ as shown in Figure 5.

In embedding I of Figure 5, both $x$ and $y$ are Möbius walks, so by Proposition 2.2.2, both $\alpha_g(x)$ and $\alpha_g(y)$ have even order. Lemma 3.3.3(1) then tells us that we have $\alpha_g(x), \alpha_g(y) \in \{g, \pm 1\}$, which implies that $\alpha_g(x) + \alpha_g(y) \in \{g \pm 1, 0, \pm 2\}$. However this contradicts the fact that $xy$ is a facial boundary walk and hence, by Lemma 3.3.3(1), $\alpha_g(x) + \alpha_g(y) \in \{\pm 1\}$.

In embedding II of Figure 5, $x$ is a Möbius walk and $y$ is a facial boundary walk, so Lemma 3.3.3(1) with Proposition 2.2.2 tells us that $\alpha_g(x), \alpha_g(y) \in \{g, \pm 1\}$. Together, we see that $\alpha_g(x) + \alpha_g(y) \in \{g \pm 1, 0, \pm 2\}$, which contradicts the fact that since $xy$ is also a Möbius walk it must be that $\alpha_g(x) + \alpha_g(y) \in \{g, \pm 1\}$.

In summary, we see that no rotation family has $(k, \breve{g}, ag+b) = (2, \frac{1}{2}, 2g)$.

**Case** $(k, \breve{g}, ag+b) = (2, 1, g)$**:**

Since $\breve{g} = 1$, the surface $\breve{S}$ is either the torus $\mathbf{T}$ or the Klein bottle, but because $ag + b = g$ can be odd, by Observation 3.3.4 we must have $\breve{S} = \mathbf{T}$. Because $k = 2$ we require our embedding to be an irreducible 2-face embedding, namely an embedding of $B_3$ in $\mathbf{T}$; the only such embeddings are shown in Figure 2.

In embedding I the facial boundary walks are $z$ and $xyx^{-1}y^{-1}z$. Because each face contains a branch point, the total voltage on each face is a generator in $\mathbb{Z}_g$. By Lemma 3.3.3(2) we must have $\alpha_g(x), \alpha_g(y) \in \{0, \pm 1\}$ and $\alpha_g(z) \in \{\pm 1\}$, so the possible triples $(\alpha_g(x), \alpha_g(y), \alpha_g(z))$ are the elements of $\{(\pm 1, \pm 1, \pm 1), (0, \pm 1, \pm 1), (\pm 1, 0, \pm 1), (0, 0, \pm 1)\}$. Consider the cellular automorphism defined by

$$\begin{cases} x \mapsto y \\ y \mapsto x \\ z \mapsto z^{-1} \; ; \end{cases}$$

applying Proposition 2.2.3 yields an automorphism of derived graphs. We also consider the formal mapping

$$\begin{cases} x \mapsto x \\ y \mapsto y \\ z \mapsto z^{-1} \end{cases}.$$

While this does not define a cellular automorphism it does induce an (unoriented) isomorphism of derived graphs for each $g$ since $z$ is contractible and has its ends consecutive in the rotation around the vertex of $B_3$. Finally, we mention the automorphisms of derived graphs provided by the automorphism of $A$ given by $1 \mapsto -1$ (see Proposition 2.2.3, Item 2). Using all these automorphisms together, we see that all solutions $(\alpha_g(x), \alpha_g(y), \alpha_g(z))$ are completely represented, up to automorphism, by the elements of

$$\{(1,1,1),(1,-1,1),(0,1,1),(0,0,1)\}.$$

These examples are constructed in Section 3.2 as $\mathcal{R}\big[(2,2),\ \{xy^{-1}x^{-1}z^{-1}y,z\};\ \mathbb{Z}_g,\ (1,1,1)\big]$, $\mathcal{R}\big[(2,2),\ \{xy^{-1}x^{-1}z^{-1}y,z\};\mathbb{Z}_g,\ (1,-1,1)\big]$, $\mathcal{R}\big[(2,2),\ \{xy^{-1}x^{-1}z^{-1}y,z\};\ \mathbb{Z}_g,\ (0,1,1)\big]$, and $\mathcal{R}\big[(2,2),\ \{xy^{-1}x^{-1}z^{-1}y,z\};\ \mathbb{Z}_g,\ (0,0,1)\big]$.

In embedding II the facial boundary walks are $xz^{-1}$ and $xy^{-1}z^{-1}y$. Because each face contains a branch point, the total voltage on each face is a generator in $\mathbb{Z}_g$. By Lemma 3.3.3(2) we must have $\alpha_g(x), \alpha_g(y), \alpha_g(z) \in \{0, \pm 1\}$ and $\alpha_g(x) - \alpha_g(z) \in \{\pm 1\}$, so the possible triples $(\alpha_g(x), \alpha_g(y), \alpha_g(z))$ are the elements of $\{(\pm1,\pm1,0),\ (0,\pm1,\pm1),\ (\pm1,0,0),\ (0,0,\pm1)\}$. Considering the cellular automorphisms defined by

$$\begin{cases} x \mapsto x^{-1} \\ y \mapsto y \\ z \mapsto z^{-1} \end{cases} \quad \text{and} \quad \begin{cases} x \mapsto z \\ y \mapsto y^{-1} \\ z \mapsto x \end{cases},$$

respectively, and applying Proposition 2.2.3, we see that these solutions are completely represented, up to automorphism, by

$$(\alpha_g(x), \alpha_g(y), \alpha_g(z)) \in \{(1,1,0),(1,-1,0),(1,0,0)\}.$$

These are constructed in Section 3.2 as $\mathcal{R}\big[(2,2),\ \{xy^{-1}z^{-1}y, x^{-1}z\};\mathbb{Z}_g,\ (1,1,0))\big]$, $\mathcal{R}\big[(2,2),\ \{xy^{-1}z^{-1}y, x^{-1}z\};\ \mathbb{Z}_g,\ (1,-1,0)\big]$, and $\mathcal{R}\big[(2,2),\ \{xy^{-1}z^{-1}y, x^{-1}z\};\ \mathbb{Z}_g,\ (1,0,0)\big]$.

In embedding III the facial boundary walks are $xz^{-1}y$ and $xyz^{-1}$. Because each face contains a branch point, the total voltage on each face is a generator in $\mathbb{Z}_g$. By Lemma 3.3.3(2) we must have $\alpha_g(x), \alpha_g(y), \alpha_g(z) \in \{0, \pm 1\}$ and $\alpha_g(x) + \alpha_g(y) - \alpha_g(z) \in \{\pm 1\}$, so the possible triples $(\alpha_g(x), \alpha_g(y), \alpha_g(z))$ are the elements of $\{(0,0,\pm1),\ (0,\pm1,0),\ (\pm1,0,0),\ \pm(1,1,1),\ \pm(1,-1,\pm1)\}$. Considering the cellular automorphisms defined by

$$\begin{cases} x \mapsto y \\ y \mapsto x \\ z \mapsto z \end{cases} \quad \text{and} \quad \begin{cases} x \mapsto z \\ y \mapsto x^{-1} \\ z \mapsto y \end{cases},$$

respectively, and applying Proposition 2.2.3, as well as considering the automorphisms of derived graphs provided by Proposition 2.2.3 from the automorphism of $A$ given by $1 \mapsto -1$, we see that these solutions are completely represented, up to automorphism, by $(\alpha_g(x), \alpha_g(y), \alpha_g(z)) \in \{(0,0,1),(1,1,1)\}$. These are constructed in Section 3.2 as $\mathcal{R}\big[(2,2),\ \{xz^{-1}y, x^{-1}zy^{-1}\};\ \mathbb{Z}_g,\ (1,1,1)\big]$ and $\mathcal{R}\big[(2,2),\ \{xz^{-1}y, x^{-1}zy^{-1}\};\ \mathbb{Z}_g,\ (0,0,1)\big]$.

**Case** $(k, \check{g}, ag+b) = (3, 0, 2g+1)$**:**

Since $\check{g} = 0$, the surface $\check{S}$ is the sphere $\mathbf{S}$. Because $k = 3$ we require our embedding to be an irreducible 3-face embedding, namely an embedding of $B_2$ in $\mathbf{S}$; the only such embedding is shown in Figure 3.

The facial boundary walks are $x, y$, and $xy$. Because each face contains a fixed point, the total voltage on each face is a generator in $\mathbb{Z}_{2g+1}$. By Lemma 3.3.3(3) we therefore have $\alpha_g(x), \alpha_g(y), \alpha_g(x) + \alpha_g(y) \in \{\pm g\} \cup \{\pm 2^t | t \geq 0\}$. We now deduce the possible solutions to this system of equations.

If $\alpha_g(x), \alpha_g(y) \in \{\pm g\}$ then $\alpha_g(x) + \alpha_g(y) \in \{0, \pm 2g\} = \{0, \pm 1\}$. Since $\alpha_g(x) + \alpha_g(y) = 0$ is not an option, we must have $(\alpha_g(x), \alpha_g(y)) = \pm(g, g)$.

Suppose $\alpha_g(x) \in \{\pm g\}$ and $\alpha_g(y) = 2^t$ for some $t$. Note that $2^t$ is a constant independent of $g$. We cannot have $\alpha_g(x) + \alpha_g(y) = \alpha_g(x)$, because then $2^t \equiv 0 (\operatorname{mod} 2g+1)$, which is impossible. We cannot have $\alpha_g(x)+\alpha_g(y) \in \{\pm 2^t | t \geq 0\}$, because that would imply $2|g$ for all $g$, which is also impossible. It must be, then, that $\alpha_g(x) + \alpha_g(y) = -\alpha_g(x)$. If $\alpha_g(x) = -g$, this gives $2^t \equiv 2g (\operatorname{mod} 2g + 1)$, which certainly cannot hold for large values of $g$. Thus, it must be that $\alpha_g(x) = g$, in which case $2^t = \alpha_g(y) \equiv 1 (\operatorname{mod} 2g + 1)$. Since this holds for all $g$, we have $t = 0$, and $(\alpha_g(x), \alpha_g(y)) = \pm(g, 1)$. A similar analysis reversing the roles of $x$ and $y$ shows that $(\alpha_g(x), \alpha_g(y)) = \pm(1, g)$ are also possible solutions.

Now suppose that $\alpha_g(x), \alpha_g(y) \in \{\pm 2^t | t \geq 0\}$. We cannot have $\alpha_g(x) + \alpha_g(y) \in \{\pm g\}$ since then we have $2|g$ for all $g$, a contradiction. Thus we must have a solution to $\epsilon_1 2^{t_1} + \epsilon_2 2^{t_2} \equiv \epsilon_3 2^{t_3} (\operatorname{mod} 2g+1)$ where $\epsilon_1, \epsilon_2, \epsilon_3 \in \{\pm 1\}$. Since $t_1, t_2, t_3$ and $\epsilon_1, \epsilon_2, \epsilon_3$ are all constants, but $g$ varies, we must have $\epsilon_1 2^{t_1} + \epsilon_2 2^{t_2} = \epsilon_3 2^{t_3}$. Without loss of generality we may assume $t_1 \leq t_2 \leq t_3$, so we have $\epsilon_1 + \epsilon_2 2^{t_2 - t_1} = \epsilon_3 2^{t_3 - t_1}$. Now $\epsilon_1 + \epsilon_2 2^{t_2 - t_1} = \epsilon_3 2^{t_3 - t_1}$ cannot be odd, so $t_2 = t_1$. This in turn implies $\epsilon_1 = \epsilon_2$, since otherwise $\epsilon_3 2^{t_3} = 0$, a contradiction. Thus, we obtain solutions $(\alpha_g(x), \alpha_g(y)) = \pm(2^t, 2^t)$ for all $t \geq 0$.

To sum up, the system of equations has possible solutions $(\alpha_g(x), \alpha_g(y)) \in \{\pm(g, g),\ \pm(g, 1),\ \pm(1, g)\} \cup \{\pm(2^t, 2^t) | t \geq 0\}$. Considering the cellular automorphisms defined by

$$\left\{ \begin{array}{l} x \mapsto x^{-1} \\ y \mapsto y^{-1} \end{array} \right. \quad \text{and} \quad \left\{ \begin{array}{l} x \mapsto y^{-1} \\ y \mapsto x^{-1} \end{array} \right. ,$$

respectively, and applying Proposition 2.2.3, we see that these solutions correspond, up to automorphism, to $\{(g, g), (1, g)\} \cup \{(2^t, 2^t) | t \geq 0\}$. Consider, further, the isomorphisms of $\mathbb{Z}_{2g+1}$ determined by $g \mapsto 1$ or $2^t \mapsto 1$, respectively (for all possible values of $t$). These all give isomorphic derived graphs, and thus all solutions to our system of equations are represented, up to automorphism, by the cases $(\alpha_g(x), \alpha_g(y)) \in \{(1, 1), (1, g)\}$. As described in Section

3.2, the rotation family $\mathcal{R}\big[(0,3),\ \{x,y,x^{-1}y^{-1}\};\ \mathbb{Z}_{2g+1},\ (1,1)\big]$ corresponds to $(\alpha_g(x),\alpha_g(y)) = (1,1)$, and the family $\mathcal{R}\big[(0,3),\ \{x,y,x^{-1}y^{-1}\};\ \mathbb{Z}_{2g+1},\ (1,g)\big]$ corresponds to $(\alpha_g(x),\alpha_g(y)) = (1,g)$.

**Case** $(k,\breve{g},ag+b) = (4,0,g+1)$**:**

Since $\breve{g} = 0$, the surface $\breve{S}$ is the sphere $\mathbf{S}$, and because $k = 4$ we require our embedding to be an irreducible 4-face embedding, namely an embedding of $B_3$ in $\mathbf{S}$. The two possible such embeddings are shown in Figure 4.

In embedding I of Figure 4 the facial boundary walks are $x, y, z$, and $xzy$. Because each face contains a fixed point, the total voltage on each face is a generator in $\mathbb{Z}_{g+1}$. By Lemma 3.3.3(2) we therefore have

$$\alpha_g(x), \alpha_g(y), \alpha_g(z), \alpha_g(x)+\alpha_g(z)+\alpha_g(y) \in \{\pm 1\}.$$

This system of equations has six solutions:

$$(\alpha_g(x),\alpha_g(y),\alpha_g(z)) \in \left\{ \begin{array}{l} (1,1,-1),(1,-1,1),(-1,1,1), \\ (-1,-1,1),(-1,1,-1),(1,-1,-1) \end{array} \right\}.$$

Considering the cellular automorphisms defined by

$$\left\{ \begin{array}{l} x \mapsto y^{-1} \\ y \mapsto x^{-1} \\ z \mapsto z^{-1} \end{array} \right. \quad \text{and} \quad \left\{ \begin{array}{l} x \mapsto x^{-1} \\ y \mapsto z^{-1} \\ z \mapsto y^{-1} \end{array} \right. ,$$

respectively, and applying Proposition 2.2.3, we see that all six solutions correspond, up to isomorphism, to the single case $(\alpha_g(x),\alpha_g(y),\alpha_g(z)) = (1,1,-1)$, which is constructed in Section 3.2 as the family
$\mathcal{R}\big[(0,4),\ \{x,y,z,x^{-1}y^{-1}z^{-1}\};\ \mathbb{Z}_{g+1},\ (1,1,-1)\big]$.

In embedding II of Figure 4 the facial boundary walks are $x, z, yx$, and $yz$. Because each face contains a fixed point, the total voltage on each face is a generator in $\mathbb{Z}_{g+1}$. By Lemma 3.3.3(2) we therefore have

$$\alpha_g(x), \alpha_g(z), \alpha_g(y)+\alpha_g(x), \alpha_g(y)+\alpha_g(z) \in \{\pm 1\}.$$

This system of equations has six solutions:

$$(\alpha_g(x),\alpha_g(y),\alpha_g(z)) \in \left\{ \begin{array}{l} (1,-2,1),(1,0,1),(-1,2,-1), \\ (-1,0,-1),(1,0,-1),(-1,0,1) \end{array} \right\}.$$

We reject the solutions with $\alpha_g(y) = \pm 2$ since these fail to satisfy the conclusion of Lemma 3.3.3(2). Considering the cellular automorphism defined by

$$\left\{ \begin{array}{l} x \mapsto x^{-1} \\ y \mapsto y^{-1} \\ z \mapsto z^{-1} \end{array} \right. ,$$

and applying Proposition 2.2.3, we see that the remaining solutions correspond, up to isomorphism, to the cases

$$(\alpha_g(x),\alpha_g(y),\alpha_g(z)) \in \{(1,0,1),(1,0,-1)\},$$

which are constructed in Section 3.2 as the families $\mathcal{R}\big[(0,4),\ \{x,yz,z^{-1},x^{-1}y^{-1}\};\ \mathbb{Z}_{g+1},\ (1,0,1)\big]$ and $\mathcal{R}\big[(0,4),\ \{x,yz,z^{-1},x^{-1}y^{-1}\};\ \mathbb{Z}_{g+1},\ (1,0,-1)\big]$. $\square$

## 4. Rotation Families with No Fixed Point

### *4.1. Preliminary Analysis*

In Proposition 3.3.1 we observed that it is numerically possible to have $k = 0$. Here, we do a preliminary analysis of those cases.

**Theorem 4.1.1.** *If a rotation family has no fixed points, then it is an order $g-1$ cellular automorphism of the genus $g$ surface, with quotient $\check{S}$ equal to the double torus $\mathbf{T^2}$.*

There do exist cellular automorphisms as described in Theorem 4.1.1; Figure 8 depicts an order 3 cellular automorphism of the genus 4 surface having no fixed points and whose quotient is $\mathbf{T^2}$. Construction of such cellular automorphisms is discussed briefly in Section 4.2.

**Lemma 4.1.2.** *Under the hypotheses of Theorem 4.1.1, if $a, ac$, and $ac^3$ are Möbius walks or if $ab, abc$, and $abc^3$ are Möbius walks, then $\alpha_g(a) \in \{\pm 1, g-1\}$ and $\alpha_g(c) = 0$.*

*Proof.* We consider the case that $a, ac$, and $ac^3$ are Möbius walks; the other case readily follows by an analogous argument. By Proposition 2.2.2 we know that the respective total voltages

$$\alpha_g(a), \alpha_g(a) + \alpha_g(c), \text{ and } \alpha_g(a) + 3\alpha_g(c)$$

must all have even order, and Lemma 3.3.3(1) tells us that each of these has total voltage in $\{\pm 1, g-1\}$. As a result, we have

$$\alpha_g(c) = \big(\alpha_g(a) + \alpha_g(c)\big) - \alpha_g(a) \ \in \{0, \pm 2, \pm g\}$$

and

$$3\alpha_g(c) = \big(\alpha_g(a) + 3\alpha_g(c)\big) - \alpha_g(a) \ \in \{0, \pm 2, \pm g\}.$$

This can only hold for all $g \geq g_0$ if $\alpha_g(c) = 0$. □

*Proof. (Of Theorem 4.1.1).*

We consider the two possible cases from Proposition 3.3.1.

**Case** $(k, \check{g}, ag+b) = (0, \frac{3}{2}, 2g-2)$**:**

Since $\check{g} = \frac{3}{2}$, the surface $\check{S}$ is Dyck's (3-crosscaps) surface $\mathbf{D}$. Because $k = 0$ we need only a single-face embedding in $\mathbf{D}$, which requires 3 loops. We consider in turn each of the possible embeddings of $B_3$ in $\mathbf{D}$ as shown in Figure 6.

In embedding I, we have Möbius walks $x, xy$ and $xy^3$, as well as $xz$ and $xz^3$. Applying Lemma 4.1.2 twice, we have $\alpha_g(y) = \alpha_g(z) = 0$.

The single facial boundary walk in embedding I is $xy^{-1}zxzy^{-1}$, which has total voltage $2\alpha_g(x) - 2\alpha_g(y) + 2\alpha_g(z) = 2\alpha_g(x)$. Since $k = 0$, this total voltage must equal 0, forcing $\alpha_g(x) \in \{0, g-1\}$. In either case, however, the voltages on the edges do not generate $\mathbb{Z}_{2g-2}$, so the lift is not connected when $g > 2$, a contradiction.

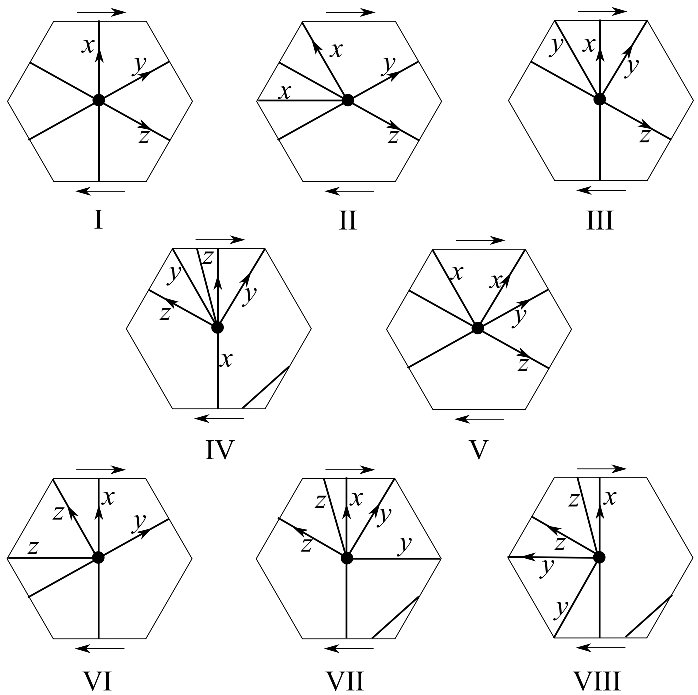


Figure 6: The eight embeddings of $B_3$ in $\mathbf{D}$. [5] As above, our convention when depicting topological surfaces is to identify opposite sides of a polygon, and to do this in an orientation-preserving manner unless there are arrows indicating otherwise.

In embedding II we have Möbius walks $x, xz^{-1}$, and $xz^{-3}$. By Lemma 4.1.2 these give $\alpha_g(z) = 0$. We also have Möbius walks $xz^{-1}y$ and $xz^{-1}y^3$, with total voltages $\alpha_g(x)+\alpha_g(y)$ and $\alpha_g(x)+3\alpha_g(y)$, respectively, since $\alpha_g(z) = 0$. Again applying the argument from Lemma 4.1.2, we obtain $\alpha_g(y) = 0$. Now, the single facial boundary walk in embedding II is $xz^{-1}y^{-1}zxy^{-1}$, which has total voltage $2\alpha_g(x) - 2\alpha_g(y) = 2\alpha_g(x)$. Since $k = 0$, this total voltage must equal 0, forcing $\alpha_g(x) \in \{0, g{-}1\}$. But then the voltages on the edges do not generate $\mathbb{Z}_{2g-2}$, a contradiction.

In embedding III of Figure 6 the facial boundary walk is $xz^{-1}x^{-1}y^{-1}zy^{-1}$ and the total voltage is $-2\alpha_g(y)$, and thus $\alpha_g(y) \in \{0, g{-}1\}$. Since $y$ is a Möbius walk, by Proposition 2.2.2 and Lemma 3.3.3(1) we have $\alpha_g(y) \in \{\pm 1, g{-}1\}$, so $\alpha_g(y) = g{-}1$. Now $x, xz$, and $xz^3$ are Möbius walks, so by Lemma 4.1.2 we have $\alpha_g(z) = 0$. Since $\alpha_g(x), \alpha_g(y)$, and $\alpha_g(z)$ must generate $\mathbb{Z}_{2g-2}$, it must be that $\alpha_g(x) = \pm 1$. However, we now have a contradiction, since $xyxz$ is a Möbius walk but $\alpha_g(x) + \alpha_g(y) + \alpha_g(x) + \alpha_g(z) = 2(\pm 1) + g - 1 + 0 \notin \{\pm 1, g - 1\}$.

In embedding IV of Figure 6 we have Möbius walks $x, z$, and $xz$, so by Proposition 2.2.2 and Lemma 3.3.3(1) each of $\alpha_g(x)$, $\alpha_g(z)$, and $\alpha_g(x) + \alpha_g(z)$ is an element of $\{\pm 1, g{-}1\}$, which is a contradiction.

In embedding V of Figure 6 the facial boundary walk is $xz^{-1}yzy^{-1}x$ and has total voltage $2\alpha_g(x)$, so $\alpha_g(x) \in \{0, g-1\}$. We also have Möbius walks $xz^{-1}, xz^{-1}y^{-1}$ and $xz^{-1}y^{-3}$ as well as $y^{-1}x, y^{-1}xz^{-1}$ and $y^{-1}xz^{-3}$. By Lemma 4.1.2 we know that $\alpha_g(y) = \alpha_g(z) = 0$. However, this implies that the voltages on the edges do not generate $\mathbb{Z}_{2g-2}$ when $g > 2$, hence the lift is not connected, a contradiction.

In embedding VI of Figure 6 we have Möbius walks $x, xy^{-1}$, and $xy^{-3}$, which gives us $\alpha_g(y) = 0$ by Lemma 4.1.2. The boundary walk for embedding VI is $xy^{-1}x^{-1}z^2y^{-1}$ and has total voltage $2\alpha_g(z) - 2\alpha_g(y) = 2\alpha_g(z)$, which must be 0, so $\alpha_g(z) \in \{0, g–1\}$. But $z$ itself is a Möbius walk, so that $\alpha_g(z) \in \{\pm1, g–1\}$, which gives $\alpha_g(z) = g - 1$. Now $x$ is also a Möbius walk so $\alpha_g(x) \in \{\pm1, g–1\}$, but since $\alpha_g(x), \alpha_g(y)$, and $\alpha_g(z)$ must generate $\mathbb{Z}_{2g-2}$ it must be that $\alpha_g(x) = \pm1$. This leads to a contradiction since $xz^{-1}x$ is a Möbius walk and therefore $2\alpha_g(x) + \alpha_g(z) = 2(\pm1) + g - 1 \in \{\pm1, g–1\}$, which is not possible.

In both embedding VII and VIII we have Möbius walks $x, y$, $x^2y^{-1}$, $x^2z$, $xy^{-1}z$, and $z^2x$, and thus each of

$$\begin{array}{lll} \alpha_g(x), & 2\alpha_g(x) - \alpha_g(y), & \alpha_g(x) - \alpha_g(y) + \alpha_g(z), \\ \alpha_g(y), & 2\alpha_g(x) + \alpha_g(z), & \text{and } \ 2\alpha_g(z) + \alpha_g(x) \end{array}$$

is an element in $\{\pm1, g–1\}$. In embedding VII the single facial boundary walk is $xy^{-2}xz^2$ and in embedding VIII it is $x^2y^{-2}z^2$, but in both the facial boundary walk has total voltage $2\alpha_g(x) - 2\alpha_g(y) + 2\alpha_g(z)$ which, because $k = 0$, equals 0, and thus $\alpha_g(x) - \alpha_g(y) + \alpha_g(z) \in \{0, g-1\}$. As noted above, however, $\alpha_g(x) - \alpha_g(y) + \alpha_g(z) \in \{\pm1, g-1\}$, so $\alpha_g(x) - \alpha_g(y) + \alpha_g(z) = g - 1$.

Consider the options in $\alpha_g(x) = \{\pm1, g-1\}$ separately. Suppose first that $\alpha_g(x) = 1$. Then since $2 - \alpha_g(y) = 2\alpha_g(x) - \alpha_g(y) \in \{\pm1, g-1\}$ we get $y \in \{1, 3, 3-g\}$. But $\alpha_g(y) \in \{\pm1, g-1\}$ as well, so $\alpha_g(y) = 1$. Therefore $\alpha_g(z) = \alpha_g(x) - \alpha_g(y) + \alpha_g(z) = g-1$. This in turn gives $2\alpha_g(x) + \alpha_g(z) = g+1$, contradicting the fact that $x^2z$ is a Möbius walk.

The analysis for $\alpha_g(x) = -1$ is essentially the same; we deduce that $\alpha_g(y) = -1$ and $\alpha_g(z) = g - 1$, and obtain the contradiction $2\alpha_g(x) + \alpha_g(z) = g - 3$.

Finally, suppose that $\alpha_g(x) = g - 1$. Since $\alpha_g(x) - \alpha_g(y) + \alpha_g(z) = g - 1$ we obtain $\alpha_g(z) = \alpha_g(y)$. Now $\alpha_g(y) \in \{\pm1, g-1\}$, but if $\alpha_g(z) = \alpha_g(y) = g - 1$ then the voltages on the edges won't generate $\mathbb{Z}_{2g-2}$, a contradiction. Thus $\alpha_g(z) = \alpha_g(y) = \pm1$. This gives $\pm2 + g - 1 = 2\alpha_g(z) + \alpha_g(x) \in \{\pm1, g–1\}$, also a contradiction.

In summary, we see that no rotation family has $(k, \breve{g}, ag + b) = (0, \frac{3}{2}, 2g - 2)$.

**Case** $(k, \breve{g}, ag + b) = (0, 2, g–1)$**:**

Since $\breve{g} = 2$, the surface $\breve{S}$ is either the genus two surface ("double torus") $\mathbf{T^2}$ or the 4-crosscaps surface. However, $g - 1$ can be odd, so by Observation 3.3.4 we must have $\breve{S} = \mathbf{T^2}$. □

It is now possible to construct a catalog as in Section 3.2 and to prove its completeness, as in Section 3.3. Since there are no fixed points, an irreducible

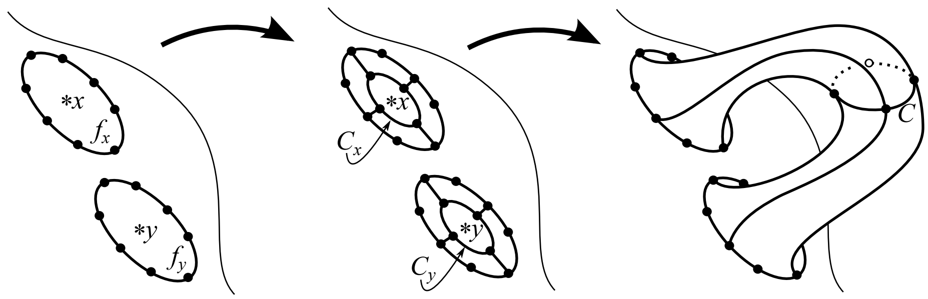


Figure 7: An illustration of the fixed-point reduction process. The points $x$ and $y$ are fixed points in faces $f_x$ and $f_y$, respectively, and the cycles $C_x$ and $C_y$ are identified to form $C$.

embedding in $\mathbf{T^2}$ is an embedding of the 4-loop bouquet $B_4$. Jackson and Visentin [5] identify four such embeddings of $B_4$ in $\mathbf{T^2}$. Because these are all one-face embeddings in which each edge appears once in each direction, there are very few constraints a voltage assignment must satisfy; it is easy to see that there are many possible voltage assigments. It seems, therefore, that the key task would be to identify the isomorphism classes of embeddings. While constructing and proving the completeness of a catalog of rotation families with $k = 0$ is doable, perhaps with computer assistance, here we content ourselves with briefly sketching an alternative approach.

*4.2. Alternative Approach*

Suppose $\varphi$ is an order $n$ fixed-point cellular rotation, with $k$ fixed points, of a graph $G$ in an orientable genus $g$ surface $S$. Let $x, y$ be distinct fixed points of $\varphi$; by [3, Theorem 4.3.7] these exist, and by definition of cellular rotation $x$ and $y$ are the centers of some faces $f_x, f_y$ respectively. Choose a vertex $u_x$ in $\partial f_x$, attach a new pendant edge to each of $u_x, \varphi(u_x), \ldots, \varphi^{n-1}(u_x)$, and connect the newly created pendant vertices in sequence with an $n$-cycle $C_x$ in $f_x$ so that $x$ is surrounded by $C_x$. Similarly, chose a vertex $u_y$ in $\partial f_y$ and add a new $n$-cycle $C_y$ in $f_y$.

Removing the faces bounded by $C_x$ and $C_y$ and identifying $C_x$ with $C_y$ according to the mapping sending $\varphi^k(u_x) \mapsto \varphi^k(u_y)$ for each $k$ yields an embedding of a graph $G'$ in a surface $S'$ of Euler characteristic $2 - 2(g + 1)$. If $S'$ is orientable, the action of $\varphi$ on $S$ induces an order $n$ cellular rotation $\varphi'$, with $k - 2$ fixed points, of $G'$ in $S'$. See Figure 7 for an illustration of this fixed-point reduction process. Note that the automorphism $\varphi'$ will not be irreducible, even if $\varphi$ was.

If $k$ is even, iterating this fixed-point reduction process $k/2$ times yields a free action on a surface of Euler characteristic $2 - 2(g + k/2)$; in the cases of the the cellular rotations in Section 3.2 having two or four fixed points the resulting surface is orientable. See Figure 8 for an example. (In the three fixed-point case, the result has only one fixed point, and is necessarily nonorientable.) The

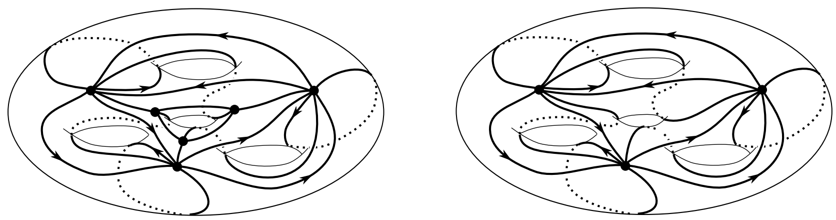

Figure 8: On the left, the result of applying the fixed-point reduction process to the order 3 cellular automorphism $\mathcal{R}\big[(1,2),\ \{xy^{-1}x^{-1}z^{-1}y,z\};\ \mathbb{Z}_g,\ (0,1,1)\big]$ depicted in Figure 9. On the right, an irreducible order 3 cellular automorphism with no fixed points which is an orbit minor of the example on the left.

obvious question now is whether all of the desired order $g-1$ fixed-point free cellular automorphisms as in Proposition 4.1.1 arise in this manner.

Suppose then that $\varphi$ is a cellular rotation with $k$ fixed points of graph $G$ in genus $g$ surface $S$, and that $C$ is a cycle in $G$ which is invariant under the $\varphi$-action and which represents a non-trivial homology class in $S$. Cutting $S$ along $C$ yields a twice-punctured surface $S'$; we view the boundaries of the closure of $S'$ as being covered by two copies of $C$, call them $C_1$ and $C_2$, respectively. Gluing in disks to close the punctures in $S'$ yields a closed surface on which $\varphi$ naturally acts; and the new faces with boundary cycles $C_1$ and $C_2$ each contain a fixed point. This resulting surface has genus $g-1$ and the $\varphi$-action has $k+2$ fixed points.

The details of this approach, including an analysis of the combinatorial structures that arise from these operations, will be pursued elsewhere.

*Acknowledgements.* The author thanks David Richter for assisting with visualizing the automorphisms in Figure 12, and anonymous referees for generously offering many useful suggestions for improving the exposition.

[1] Lowell Abrams and Daniel Slilaty. Cellular automorphisms and self-duality. *Trans. Amer. Math. Soc.*, 367(11):7695–7773, 2015.

[2] Lowell Abrams and Daniel Slilaty. The minimal $\mathbb{Z}_n$-symmetric graphs that are not $\mathbb{Z}_n$ spherical. *European J. Combinatorics*, 46:95–114, 2015.

[3] J. L. Gross and T. W. Tucker. *Topological Graph Theory*. Wiley-Interscience Series in Discrete Mathematics and Optimization. John Wiley & Sons Inc., New York, 1987. A Wiley-Interscience Publication.

[4] Pavol Gvozdjak and Jozef Širáň. Regular maps from voltage assignments. In *Graph Structure Theory (Seattle, WA, 1991)*, volume 147 of *Contemp. Math.*, pages 441–454. Amer. Math. Soc., Providence, RI, 1993.

[5] David M. Jackson and Terry I. Visentin. *An Atlas of the Smaller Maps in Orientable and Nonorientable Surfaces.* CRC Press Series on Discrete

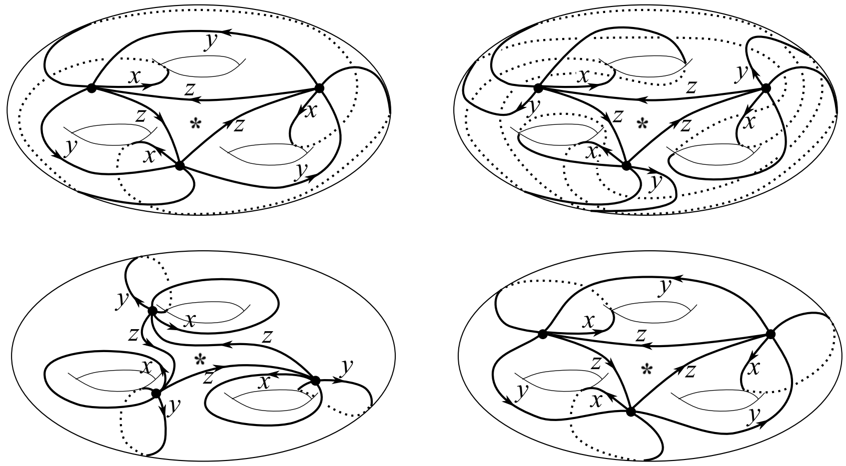


Figure 9: From upper-left proceeding clockwise, depictions of
$\mathcal{R}\big[(1,2),\ \{xy^{-1}x^{-1}z^{-1}y, z\};\, \mathbb{Z}_3,\ (1,1,1)\big]$,
$\mathcal{R}\big[(1,2),\ \{xy^{-1}x^{-1}z^{-1}y, z\};\, \mathbb{Z}_3,\ (1,-1,1)\big]$,
$\mathcal{R}\big[(1,2),\ \{xy^{-1}x^{-1}z^{-1}y, z\};\, \mathbb{Z}_3,\ (0,1,1)\big]$,
and $\mathcal{R}\big[(1,2),\ \{xy^{-1}x^{-1}z^{-1}y, z\};\, \mathbb{Z}_3,\ (0,0,1)\big]$,
with quotient given by embedding I in Figure 2.

Mathematics and its Applications. Chapman & Hall/CRC, Boca Raton, FL, 2001.

[6] T. Zaslavsky. Biased graphs. I. Bias, balance, and gains. *J. Combin. Theory Ser. B*, 47(1):32–52, 1989.

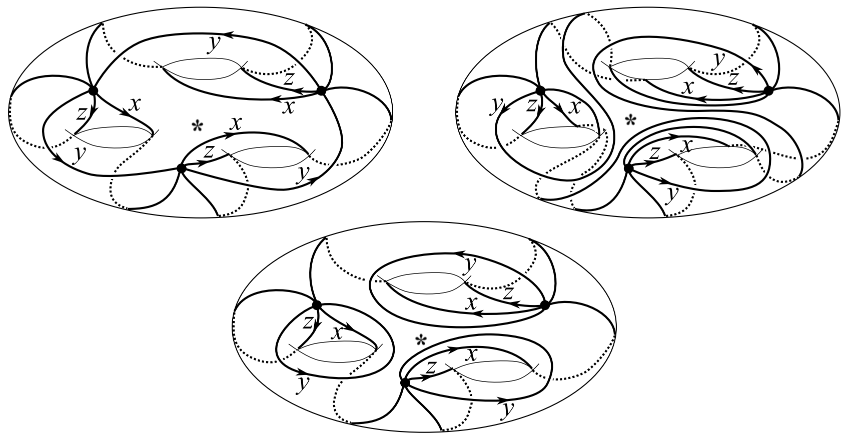

Figure 10: From upper-left, clockwise, proceeding clockwise, depictions of $\mathcal{R}\big[(1,2),\ \{xy^{-1}z^{-1}y, x^{-1}z\};\ \mathbb{Z}_3,\ (1,1,0))\big]$, $\mathcal{R}\big[(1,2),\ \{xy^{-1}z^{-1}y, x^{-1}z\};\ \mathbb{Z}_3,\ (1,-1,0)\big]$, and $\mathcal{R}\big[(1,2),\ \{xy^{-1}z^{-1}y, x^{-1}z\};\ \mathbb{Z}_3,\ (1,0,0)\big]$, with quotient given by embedding II in Figure 2.

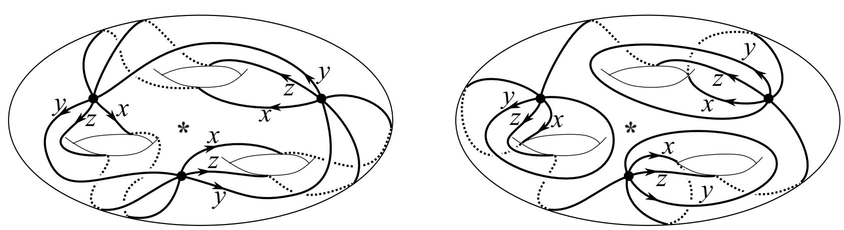

Figure 11: From left to right, depictions of $\mathcal{R}\big[(1,2),\ \{xz^{-1}y, x^{-1}zy^{-1}\};\ \mathbb{Z}_3,\ (1,1,1)\big]$ and $\mathcal{R}\big[(1,2),\ \{xz^{-1}y, x^{-1}zy^{-1}\};\ \mathbb{Z}_3,\ (0,0,1)\big]$, with quotient given by embedding III in Figure 2.

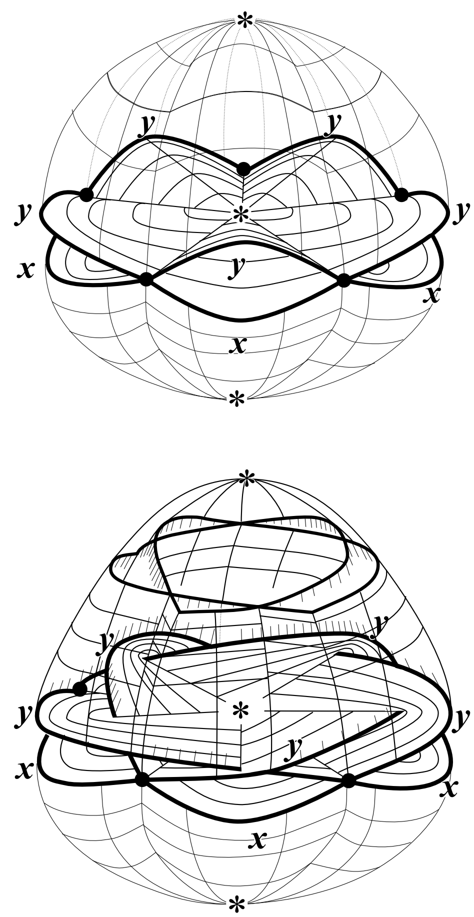

Figure 12: Depictions of the order 5 symmetries
$\mathcal{R}\big[(0,3),\ \{x,y,x^{-1}y^{-1}\};\ \mathbb{Z}_5,\ (1,1)\big]$ (above)
and $\mathcal{R}\big[(0,3),\ \{x,y,x^{-1}y^{-1}\};\ \mathbb{Z}_5,\ (1,2)\big]$ (below)
as branched immersions. The quotients are given by Figure 3. In the second depiction, a portion of the upper cap has been cut away to reveal the inner structure.

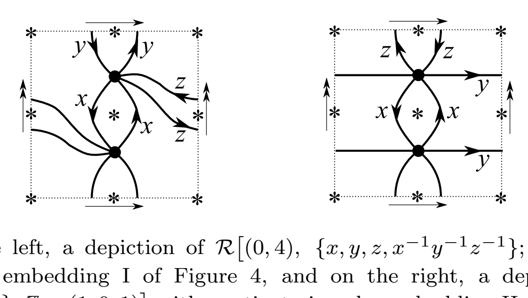

Figure 13: On the left, a depiction of $\mathcal{R}\big[(0,4),\ \{x,y,z,x^{-1}y^{-1}z^{-1}\};\ \mathbb{Z}_2,\ (1,1,1)\big]$, with quotient given by embedding I of Figure 4, and on the right, a depiction of $\mathcal{R}\big[(0,4),$ $\{x,yz,z^{-1},x^{-1}y^{-1}\};\ \mathbb{Z}_2,\ (1,0,1)\big]$ with quotient given by embedding II of Figure 4.

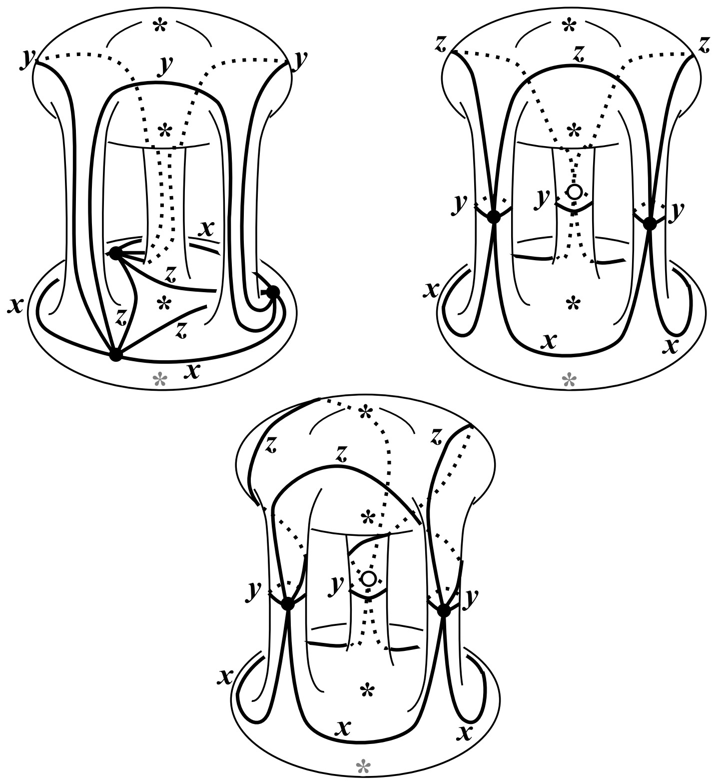


Figure 14: From upper left proceeding clockwise, depictions of
$\mathcal{R}\big[(0,4),\ \{x,y,z,x^{-1}y^{-1}z^{-1}\};\ \mathbb{Z}_3,\ (1,1,-1)\big]$,
with quotient given by embedding I of Figure 4,
and then $\mathcal{R}\big[(0,4),\ \{x,yz,z^{-1},x^{-1}y^{-1}\};\ \mathbb{Z}_3,\ (1,0,1)\big]$,
and $\mathcal{R}\big[(0,4),\ \{x,yz,z^{-1},x^{-1}y^{-1}\};\ \mathbb{Z}_3,\ (1,0,-1)\big]$,
with quotients given by embedding II of Figure 4.